



Determining a Suitable Location for Wind Turbines Using Inverse Solution and Mast Data in a Mountainous Terrain

A. H. Zare, R. Mehdipour*, E. Mohammadi

Department of Mechanical Engineering, Tafresh University, Tafresh, Iran

ABSTRACT: Optimum design of a wind farm will ensure high output rated power and low operating costs. The aim of this study was to determine the optimum location to install a wind turbine in a mountainous terrain using computational fluid dynamics. This purpose is achieved by employing inverse method, with the objective of maximizing the efficiency of the turbines while minimizing loss expenses caused by placing them in a less optimum region. Boundary conditions are determined by steepest decent optimization method. 2-D mountain geometry alongside the mast data installed on the flat area are the references of evaluating the performance of the proposed method in this paper. Results indicated that in current turbulent flow, separation occurs in atmospheric boundary layer due to an adverse pressure gradient. Furthermore resultant pressure contours demonstrated that air flow pressure decreases over the hill and its minimum value is reported at the top of the hill, thus adverse pressure gradient happens in the back hill. Simulation results revealed a considerable difference among the power outputs of the same turbine installed at different points of the domain. Turbine performance in the initial installation point and in the point derived from the algorithm is then compared. The performance reported is nineteen times better in the new suggested location.

Review History:

Received: 7 December 2017
Revised: 11 May 2018
Accepted: 24 June 2018
Available Online: 14 July 2018

Keywords:

Wind turbine site selection
Computational fluid dynamics
Inverse solution
Optimization
Atmospheric boundary layer

1- Introduction

During the last decade of the 20th century, grid-connected wind capacity worldwide has doubled approximately every three years. Due to the fast market development, wind turbine technology has experienced an important evolution over time. Wind power is the fastest growing energy technology at the turn of the millennium, and will continue to grow for the foreseeable future due to it is abundant, domestic, inexhaustible and clean energy source [1].

This rapid growth requires an extensive search for locations suitable for wind energy production. On the one hand, topographical aspects and legal frame conditions play an important role, but local wind conditions and timing decide about the financial success of a wind farm project [2]. It is also necessary to have access to detailed information about the distribution of intensity and direction of wind when determining the optimum location to build a wind farm. The ideal location should provide a relatively uniform and non-turbulent wind flow throughout the year, without sudden and sever turbulences [3-5].

Different computer methods have been introduced for simulating the atmosphere and wind conditions of a region, including linear and nonlinear models such as Yan et al. [6] and Desmond et al. [7]. The linearization of the governing equations over the atmosphere is performed by neglecting complex roughness and assuming that the terrain is uniform, consequently it has very low accuracy in the regions where the windflow is highly turbulent and has experienced separations or vortices. To avoid this problem and yet to be able to use the computer simulations for rugged and complex

terrains, it is necessary to use a far more precise model such as Computational Fluid Dynamics (CFD) [8].

In problems where one of the boundary conditions is unknown, for example the velocity inlet, inverse methods could come to handy. Determining the objective function and convergence criteria is one of the most important steps in inverse methods. Ertürk et al. [9], Mehdipour et al. [10, 11] have discussed on determining the objective function. Coupling inverse method with neural networks method [12-14], with colony system-based optimization methodology [15] or with hybrid optimization algorithm [16] has been successful to improve its performance. As the use of inverse or optimization methods in modeling the atmospheric flow has been limitedly discussed in the literature, this issue is more focused in this study.

As examples for using finite volume method in CFD application, the studies of Kim et al. [17, 18] could be pointed out. They first numerically and experimentally investigated the wind flow over 2-D hilly terrain, and then on the latter study they performed the numerical simulation by solving Reynolds-Averaged Navier-Stokes (RANS) equations. The numerical model developed for their work was based on the finite-volume method and the SIMPLEC algorithm. They indicated that flow separation occurs in the hill slope of 0.5, and the low-Reynolds-number model with an orthogonal grid is found to predict the separated flow better than the other turbulence models [17]. However their results cannot be very accurate since they didn't consider the effects of stratification of the atmosphere and pollutant-transport equations were missed.

Another study of 2-D and 3-D simulations for analysis of flow around a hill can be found in Ing and Fallo [19] study.

Corresponding author, E-mail: mehdipour@tafreshu.ac.ir

In his thesis the evaluation of wind energy resources over a site in central Italy was conducted by means of the CFD code WindSim. He showed that Root-Mean-Square (RMS) errors of velocity profiles exhibit a direct relation with the mean velocity of the directional sector, hereby showing a strong dependence on thermal effects. These effects were not taken into account by the CFD simulations. Ing and Fallo [19] found the best agreement for sectors where mean velocity is high and thermal effects were negligible.

In 2009, Russell [8] proved how a well-designed CFD model can accurately replicate the speed, direction, and turbulence at any point of a wind farm using a fixed location source data. He has claimed that “a CFD model of an operating wind farm, coupled with a local wind forecast, can increase the accuracy of predictions about producing electrical power and give out precious information to electric grid managers and wind farm operators” [8].

From the previous studies in which the Atmospheric Boundary Layer (ABL) was investigated, Fang et al. [20] and Cao et al. [21] studies could be highlighted. Fang et al. [20] modeled neutral atmospheric boundary layer based on standard k- ϵ turbulent model. Modified wall function was employed in modeling wind field of a region and moreover was experimentally examined in a wind tunnel. Cao et al. [21] investigated turbulent atmospheric boundary layer over 2-D hills with and without surface roughness by using Large-Eddy Simulation (LES) method. They showed that generation of inflow turbulence and modeling the effects of roughness blocks play important roles in simulating the turbulent boundary layer over hills. They also indicated that the reattachment point extended further downstream when the hill was rough.

Speaking about LES method, in a recent study, Liu et al. [22] studied turbulent flow fields over a 3-D hill and a 2-D ridge with smooth ground by numerically simulating wind tunnel using LES. They have stated an interesting finding in their paper; “spectra of the flow in the wake of 3-D hill are not sensitive to the turbulence condition of the oncoming flow, but 2-D ridge is” [22].

The first approach that used the genetic algorithm in optimization was made by Mosetti et al. [23], and then Grady et al. [24] wrote a computerized program that used genetic algorithm in MATLAB.

In this context, other studies have been conducted in recent years to make it scientifically more practical. For example in the study of Emami and Nogreh [25], a new coding approach and a novel objective function for solving the problem of wind turbine placement in wind farm using genetic algorithms have been introduced which led to noticeably improved results in comparison with previous works.

Wan et al. [26] introduced micro-siting of wind turbines by genetic algorithms based on improved wind and turbine models. They used wind distribution functions and power evaluation models in the optimization of wind farm configurations. They were first to introduce a real velocity distribution for the wind. Their studies were performed based on a wake model to estimate the effects of wind speed decrease at the back of each turbine.

In the present study, a novel approach has been investigated in which the inverse method is coupled with CFD and optimization methods to numerically simulate the atmospheric boundary layer in a mountainous terrain. In all the previous

researches conducted in this field, a uniform velocity profile was considered while a real velocity profile based on meteorological mast data is used herein. This novel approach classifies our case as an inverse problem. The significance of this research resides in the fact that power generation companies require to have accurate predictions to be able to invest in renewable energy section. Since a fraction of error in predicting wind speed or the location of turbines could have a substantial impact on power output of wind turbines and consequently on the amount of electricity generated, detailed and accurate modeling is of high importance.

2- Material and Methods

2- 1- CFD method compared to similar methods

Advanced applied-research programs for weather models such as wind energy forecasting, will increase the solution accuracy. Atmospheric models, cover a wide range of several square kilometers of grid cells. Surface details are very important in atmospheric modeling, because objects with relatively small surfaces can affect air flow driving the turbine blades. Through 30 years of studies on wind energy, it has been revealed that a very small error in wind velocity prediction will lead to millions of dollars loss. These huge financial consequences have led tendencies to computer simulations. Atmospheric computer simulation to determine a region’s wind conditions is performed using different ways, including linear and nonlinear models.

WASP method, a linear model to predict the wind in an area, is widely used for terrains with simple roughness, no complicated mountains included [19]. Linear models explain the flow behavior in an area, neglecting the complex roughness and assuming the terrain as uniform, by linearizing the answers of atmospheric boundary layer dynamic equations. This approach is based on statistical data, therefore it does not meet acceptable accuracy in most cases. However it requires less computer power and is accompanied by higher speed of analysis and more ease of use, this method has been used more often. More accurate models such as CFD must be used for rugged terrains. Linear models are useless when the terrains contain too much complexity and roughness. CFD methods are recommended in these cases and numerical methods for atmospheric simulation are used to predict the windflow. Application of CFD to assess wind resources has been a successful alternative to conventional methods such as WASP in recent years. The great advantage of CFD models is that they are theoretically compatible with some nonlinear effects in wind surface flow. This is more obvious when dealing with complex terrains, forests, and other places with obstacles. Also, some CFD models can cope with the effects of heat and layering. Results from CFD methods are highly dependent on the skills of the researcher.

2- 2- Simulation and gridding

The method presented in this study is somehow a novel approach. The performance of the proposed method on a conventional 2-D geometry is investigated before applying it to the actual geometry. The 2-D geometry is a hill in a plain space and a hypothetical building is placed between the inlet and the hill as shown in Fig. 1. Base velocity should be considered in the point of meteorological mast. The geometric characteristics of simulated dimensionless region are described in Table 1. The actual dimensions of the area

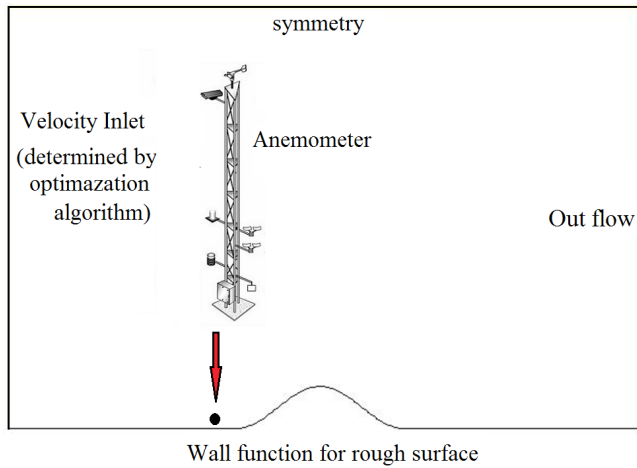


Fig. 1. The 2-D geometry of the problem

Table 1. The dimensions of the simulated geometry

The characteristics	The dimensionless Scales
Length	3
Height	2
The height of the hill	0.2

are of a height of 1 kilometer and a length of 6 kilometers while the height of the hill is 100 meters. The building has a height of 20 meters and an anemometer is installed on it.

In order to perform the simulation, the geometry was created with 61200 highly uniform quadrilateral cells and gridded by a factor of 2. Fig. 2 shows a general view of the grid.

Many studies on providing appropriate boundary conditions to simulate the atmospheric boundary layer have been conducted and some are still ongoing. The main challenge is to provide suitable boundary conditions for top and the inlet section in such a way to model atmospheric boundary layer as close as possible to reality. In this study, according to the introduced novel algorithm and inverse solution, boundary condition at the inlet is considered as velocity inlet. Symmetry boundary condition is defined for the top section [19], however the aim of this study was to discuss on the process of optimization in order to find the optimum boundary condition at the inlet.

Table 2. Estimated Values of the surface roughness and wind flow characteristics [29].

$H_o=Z_o=$ Effective surface roughness	Representative value of H_o (m)	Terrain	Power law exponent (n)	Turbulence intensity at 10 m elevation
0.5-1.5	0.7	Center of large towns, cities, forests	0.35	34
		Dense forests of relatively non-uniform height	0.27-0.30**	34
		Dense forests of relatively uniform height	0.23-0.25**	34
0.15-0.5	0.3	Small towns, suburban area	0.24	26
0.05-0.15	0.1	Wooded country villages, outskirts of small towns, farmlands	0.20	21
0.007-0.015	0.01	Grass, very few trees	0.15	14
0.0015-0.007	0.003	RUNWAY AREAS (Average) surface covered with snow rough sea in storm	0.13	13
<0.0015	0.001	Calm open sea, lakes, snow covered flat terrain, flat desert	0.11	11

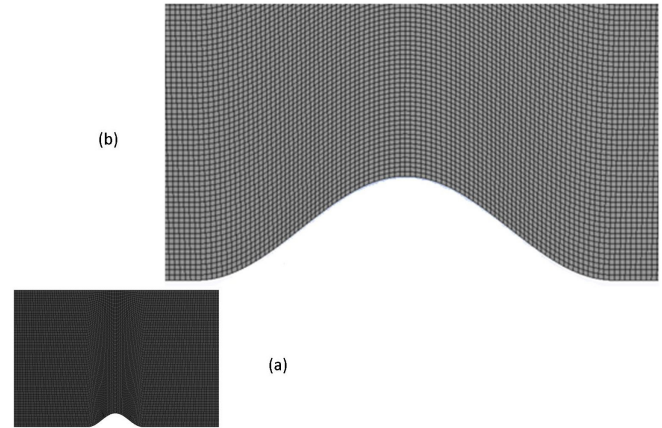


Fig. 2. The grid of the geometry: (a) the original geometry (b) magnified

2- 3- The governing equations

Natural geographical features consist of landforms and ecosystems. For example, terrain types, and physical factors of the environment are natural geographical features. Wind velocity profile is highly dependent on the terrain features. Therefore the assumptions regarding the effects of the terrain features on the wind must be taken into account. The wind passing over the earth is affected by the surface roughness which results in formation of a specific boundary layer.

Meteorological organizations usually report wind velocity using meteorological masts every 3 seconds in the altitudes of 10 m, 20 m, and 30 m.

Eq. (1) is used to determine the velocity profile in the altitudes where the masts are installed [27, 28].

$$u_{mean} / u_{ref} = (z / z_{ref})^n \quad (1)$$

where u_{ref} is the wind velocity recorded by the masts and z_{ref} is the altitude of the masts. "n" can be found based on the terrain roughness [27]. Classification of different terrains and their corresponding effects on the flow profile is shown more specifically in Table 2 [29].

Table 2 shows several measures of the characteristics of the wind including turbulence intensity. This table shows that turbulence intensity at 10 m elevation varies from about 10

percent for wind flow over water to over 20 percent for a typical suburban area [29]. According to the above table, as the studied terrain is located in a mountainous small city, the turbulence intensity will be considered 34%.

The value of “*n*” is suggested as 0.35 according to Table 2. Considering the altitude of the mast as 10 m, and “*n*” as 0.35, Eq. (1) could be written as follows.

$$u_{mean} = 0.45u_{ref} z^{0.35} \quad (2)$$

Above profile is used as inlet boundary condition of atmospheric boundary layer simulation and will help reduce the computation time.

In this study, wind profile proposed by Kim et al. [17] is considered to investigate different wind velocity profiles in atmospheric boundary layer. They introduced Eq. (3) as the velocity inlet boundary condition.

$$u(z) = \frac{u_*}{k} \log\left(\frac{z}{z_0}\right) \quad (3)$$

where u_* and terrain altitude are 0.33 m/s and 0.05 mm respectively. K is the Von Karman constant equal to 0.41.

The equations needed to calculate velocity and pressure fields will be introduced after solving governing equations for each domain and determining the velocity inlet profile.

Continuity and Navier-Stokes equations for turbulent flow should be solved to find wind velocity and pressure in each point of the domain. These equations are defined as follows.

$$\frac{\partial \rho}{\partial t} + \nabla \cdot (\rho \vec{v}) = 0 \quad (4)$$

$$\frac{\partial}{\partial t} (\rho \vec{v}) + \nabla \cdot (\rho \vec{v} \vec{v}) = -\nabla p + \nabla \cdot (\bar{\tau}) + \rho \vec{g} + \vec{F} \quad (5)$$

Velocity vectors and stress tensors are marked with \vec{v} and $\bar{\tau}$ notations in Eqs. (4) and (5) while stress tensor is defined as follow.

$$\bar{\tau} = \mu \left[\nabla \vec{v} + \nabla \vec{v}^T \right] - \left(\frac{2}{3} \right) \nabla \cdot \vec{v} I \quad (6)$$

μ is dynamic viscosity coefficient and “ I ” is the identity matrix. The anemometer is engaged with the turbulent flow field. $k-\epsilon$ model is used to simulate turbulent dynamic viscosity, since the air flow in the atmospheric boundary layer is a kind of turbulent flow. In other words, two more equations will be added to above equations to determine turbulent dynamic viscosity. The flow in the atmospheric boundary layer is incompressible as the fluid is air the thermal effects have been neglected [29].

In this approach, velocity distribution in the element can be obtained by applying sublayer correlations of turbulent flow rather than using linear relations. In this study, $y^+ < 60$ is considered to model the sublayer thickness.

2- 4- Optimization method

In this study, the inlet boundary condition is unknown since

the wind velocity is unknown there. However it is available in the mast. Such problems are classified as inverse problems. Forward, inverse and optimization method are three methods for finding these unknown parameters. All of these methods are classified as inverse problems. In our case, the purpose is to determine the velocity inlet profile. In such a way that it can replicate the recorded velocity by the mast.

In Forward method, the engineer makes essential changes in the scheme or the boundary conditions out of his own experience or the previous results from modeling. He runs the model with the new conditions and repeats this procedure until the favorable result is obtained. This method is very time-consuming and could be impossible to use in problems with too many parameters [30]. Nowadays, with growing power of computers, inverse methods are more popular among researchers and many papers have been published in this context

Eventually the inverse solution will end to a matrix. The answer will be found by inverting this matrix. The most important challenge is ill-posedness of inverse problems. Inequality in the number of equations and variables will make resolving the final matrix very difficult and sometimes impossible.

In some cases, there is no answer to problem because of the boundary conditions; therefore regularization plays an important role in inverse problems.

Optimization methods are somehow similar to Forward methods. In which the model will be running and then the design parameters will be corrected based on the simulation results.

In optimization method, the correction is performed using an objective function and the experience of the researcher could be useful only in well-defining this function.

This procedure will continue until all the design criteria are met and the objective function is minimized.

The first step is to define an objective function as $F(\varphi)$ where φ is a vector of design variables. The purpose of different optimization algorithms is to find φ^* which is able to satisfy $F(\varphi^*) = \min(F(\varphi))$.

Amongst optimization methods, Newton’s method, Quasi-Newton method (QN), Simulated Annealing Method (SAM), Ant Colony System (ACS), Genetic Algorithm (GA), Steepest-descent, Levenberg-marquardt and Conjugate gradient are the most common methods.

In this paper, steepest-descent method is employed because of its high converging speed and that no local minimum will appear in objective function. The proposed objective function is defined as follows.

$$f(\theta_r) = a_1 (V - V_{target})^2 \quad (7)$$

where V_{target} is the recorded velocity by the mast and V is the velocity derived from the simulation.

In the Steepest-descent method, design variables will be corrected in each iteration based on Eq. (8). [4] Where \vec{p}_r is search directional and a_r refers to step size.

$$\vec{\theta}_{r+1} = \vec{\theta}_r + a_r \vec{p}_r \quad (8)$$

If the minimum value of function is considered as $\vec{\theta}^*$, the value of function in each iteration as $\vec{\theta}_r$ and their connecting vector as $\vec{a}_r \vec{p}_r$, then the following equation is suggested to

find a_r ,

$$a_r = a_0 / r^a \tag{9}$$

where a_0 is a constant coefficient which can be obtained using trial and error.

In the present case, since the problem is single variable, Eq. 9 could be written as follows:

$$u_{r,i} = u_* + a_r p_r \tag{10}$$

where “r” subscript indicates the iteration; u_{r+1} and u_* are inlet velocity and wind velocity in the mast point respectively [31].

Eqs. (11) and (12) are used to find directional change to minimum point in the Steepest-descent method and they could be written as Eqs. (13) and (14) in the present study.

$$\vec{P}_r = -\vec{g}(\vec{\theta}_r) \tag{11}$$

$$g_1(\theta_r) = \frac{\partial f((\vec{\theta}_r))}{\partial \theta_r} \tag{12}$$

$$P_r = -g(V_r) \tag{13}$$

$$g(V_r) = \frac{\partial f(V_r)}{\partial v_r} \tag{14}$$

2- 5- Determination of wind specification in the region

To study the proposed algorithm, a city under extreme wind conditions is chosen which is located in a mountainous area in Iran. This city is called Tafresh and it utilizes some meteorological masts. Required data to analyze the wind specification and flow conditions is described in Table 3.

The average wind speed of Tafresh is shown in Fig. 3 throughout a period of twelve months. As it is clear in the graph, the maximum and minimum wind speed occurs in June and January respectively.

Eventually a summary of the wind characteristics in the region is given in Table 4.

Table 3. Tafresh wind specifications

Variable	Value
Latitude	N 34° 40'59.140"
Longitude	E 50° 3'26.840"
Elevation	1900 m
Start date	06/28/2010 13:30
End date	06/28/2011 15:20
Duration	9.6 months
Length of time step	10 minutes
Calm threshold	0.3 m/s
Mean temperature	11.3 °C
Mean pressure	78.93 kPa
Mean air density	0.970 kg/m ³
Power density at 50 m	69 W/m ²
Wind power class	1 (poor)
Power law exponent	0.0342
Surface roughness	5e-12 m
Roughness description	Smooth

Table 4. Tafresh wind characteristics

mean temperature	11.3 °C
Mean pressure	78.93 kPa
Mean density	0.97 kg/m ³
Average speed	3.5 m/s

2- 6- Proposed algorithm

The first step is to find the average wind speed of the region in the mast point based on the wind data recorded in recent years. The next step is to define suitable boundary conditions. Velocity inlet is one of the most important boundary conditions where in inverse method is used to choose the best velocity profile match. It's clear that Eq. (14) cannot be employed since the wind velocity is unknown in this case and consequently the corresponding derivative cannot be derived (performed); therefore a CFD code is solved for two consecutive runs. Then the velocity at the mast point is determined using the algorithm and in case of mismatch with the existing value, the boundary conditions will be corrected using Eqs. (7) to (14).

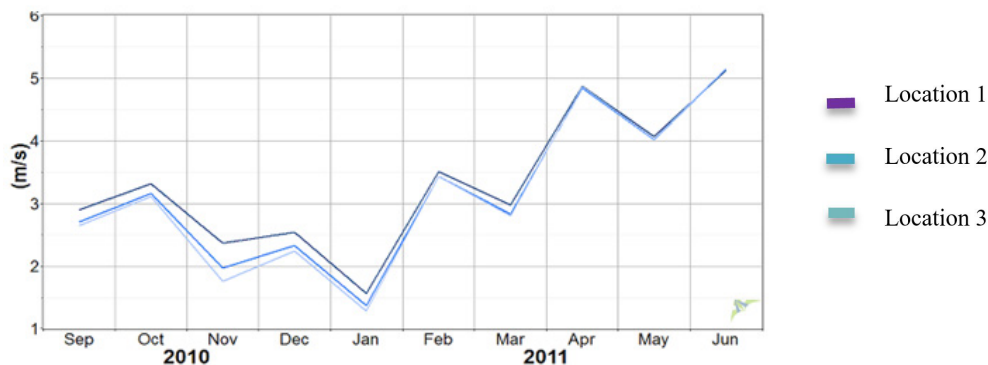


Fig. 3. Tafresh average wind speed throughout a year in three different locations

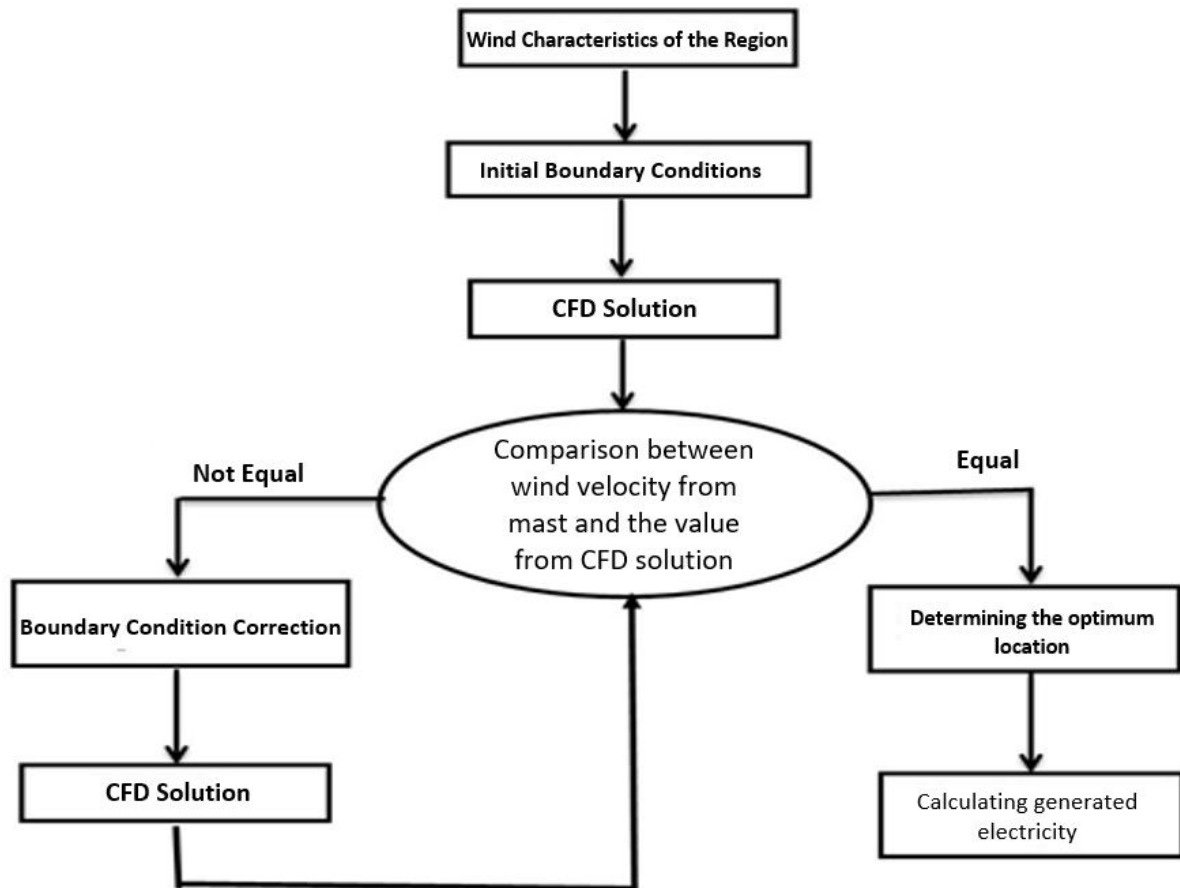


Fig. 4. Proposed algorithm

The model is solved using ANSYS FLUENT-15 solver. In this model, a code is written in the programming environment of Fluent (UDF) by applying the mentioned correlations and boundary conditions.

The optimum place to install wind turbine can be determined after defining the suitable boundary conditions and the best velocity profile match. In the present survey, aerodynamics is the only design criterion studied, although manufacturing cost, construction conditions, local roads, electricity access and etc. can be studied further but since only the 2-D geometry is investigated, adding other criteria doesn't increase the value of this work.

Determining the maximum wind speed is the basis of finding the optimum place. Turbine class and its equivalent generated electricity can be obtained according to the wind characteristics in this point. Fig. 4 illustrates the proposed algorithm in a flowchart.

3- Grid Independency and Validation

Grid independency is one of the most important steps in solving a problem using numerical method. Numerical results must be independent of the grid size. The effect of grid size on the maximum velocity is studied since the velocity is the most important parameter. The independency of results to the number of cells is demonstrated in Fig. 5. Six grids with different number of cells, 570, 1180, 27132, 61200, 94750, and 150700 cells, are investigated. It is observed that the maximum velocity remains approximately stable when the grid has more than 61200 cells.

This study has been validated by replicating the simulations

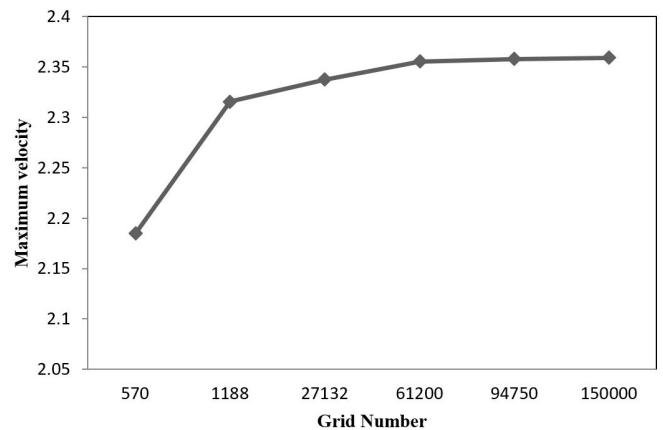


Fig. 5. Grid independency

of Kim et al. [17] and Ing and Fallo [19]. The turbulent air flow in atmospheric boundary layer over a cosine shaped hill is simulated using CFD. The cosine-shape hill has been simulated through the procedure of the CFD software, which draws the hill shape using the following equation where H is the height and L_1 is the half-length of the hill at the upwind mid-height of the hill.

$$Z = \frac{H}{2} \times \left\{ 1 + \cos \left[\left(\frac{\pi}{2} \right) \times \left(\frac{x}{L_1} \right) \right] \right\} \quad (15)$$

In current turbulent air flow in atmospheric boundary layer due to an adverse pressure gradient, separation occurs. The point where the dividing streamline, which is the flow through the central region of the recirculating flow, attaches to the wall again is called the reattachment point. The reattachment point had been taken by Ing and Fallo [19] as an important factor to compare simulations results with published simulations by Kim et al. [17]. To have a complete and reliable validation, similar method has been used in current study. The results regarding reattachment point reported by current simulations are compared with [17] and [19] in Table 5.

Table 5. Validation results

Researcher name	reattachment point
Kim et al. [17]	5.35
Ing and Fallo [19]	6.05
present study	5.58

4- Results and Discussion

Fig. 6 indicates the output of the optimization function based on the proposed code. It has been proved that the inlet velocity converges to value of 3.16 m/s. Optimization process and its different steps are presented in Table 6.

Velocity contour of the region can be obtained by the end of optimization process. The contours of the horizontal and vertical velocity components are shown in Figs. 7 and 8 respectively. Maximum velocity is observed in a point close to the top of the hill and the minimum is reported in the leeside of the hill. Static pressure contour is also illustrated in Fig. 9. Air flow pressure decreases over the hill and its minimum value is reported at the top of the hill, thus in the back hill, adverse pressure gradient exists. This is a prerequisite for separation, and if the adverse pressure gradient is large enough it will result to separation and reverse flow.

Although velocity and pressure variation can be predictable for a 2-D geometry, determining maximum velocity is quite difficult in more complex geometries. The proposed optimization algorithm can help researches solve such problems more easily.

Separation region in air flow over hill can be recognized by X velocity component contour [19]. As mentioned before, the minimum of X velocity happens at the upstream hillside. Moreover a minus value is reported in this region for X velocity which yields for reverse flow and formation of vortices. To have a better understanding from flow characteristics in separation region and to observe vortices,

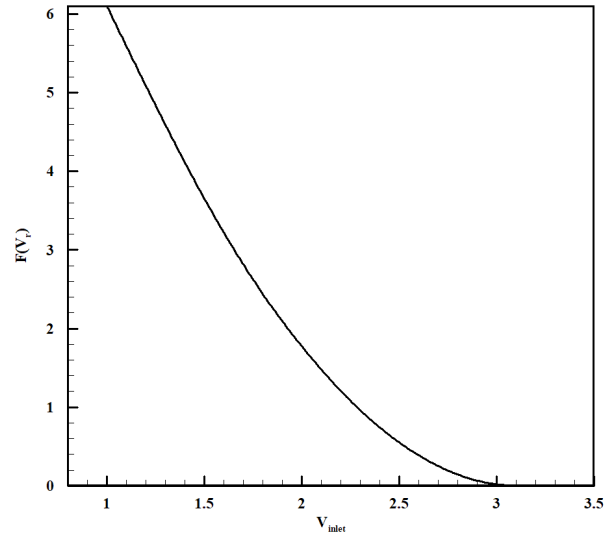


Fig. 6. The graph of the optimization function

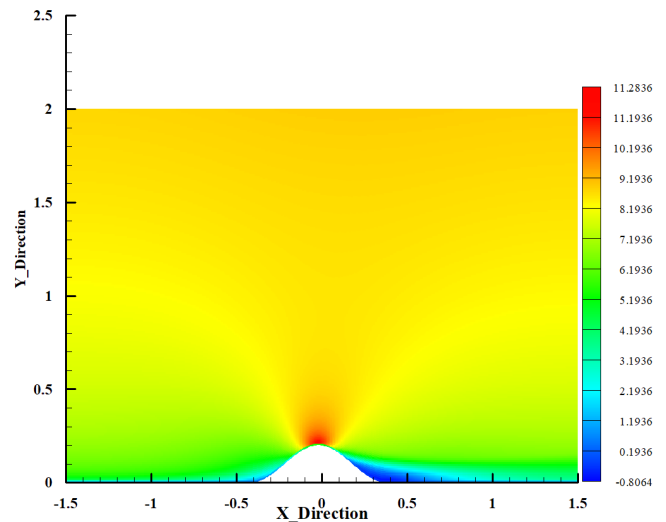


Fig. 7. X velocity component contour

Fig. 10 is presented which shows streamlines around the hill. In order to clarify the separation region in air flow over the hill, velocity vectors are also presented in Fig. 11. As it is shown in this figure, the velocity vectors are completely ordered between the hill and the entrance section, while they are highly complicated and show circulation behind the hill.

Table 6. Optimization process and calculating the objective function

V_{inlet}	$V(\text{Fluent run})$	$F(v_r)$	$G(v_r)$	$P(v_r)$	v_{r+1}	Max speed on top of the hill(m/s)
1.000	1.031	6.095	-1.415	1.415	1.783	2.490
1.500	1.590	3.648	-1.049	1.049	1.993	4.550
1.783	1.920	2.496	-1.240	1.240	2.241	5.480
1.993	2.160	1.795	-1.691	1.691	2.579	6.170
2.241	2.450	1.102	-2.250	2.250	3.029	7.004
2.579	2.853	0.418	-2.705	2.705	3.164	8.140
3.029	3.389	0.012	-3.030	3.030	3.316	9.640
3.164	3.550	0.002				10.140

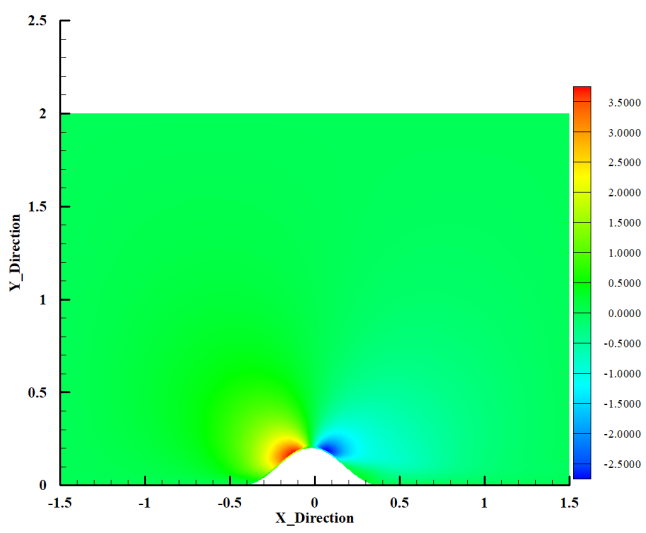


Fig. 8. Y velocity component contour

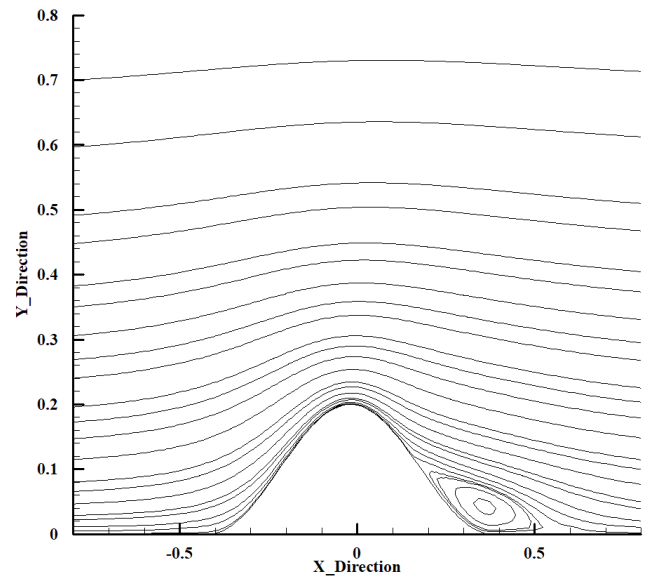


Fig. 10. Streamlines

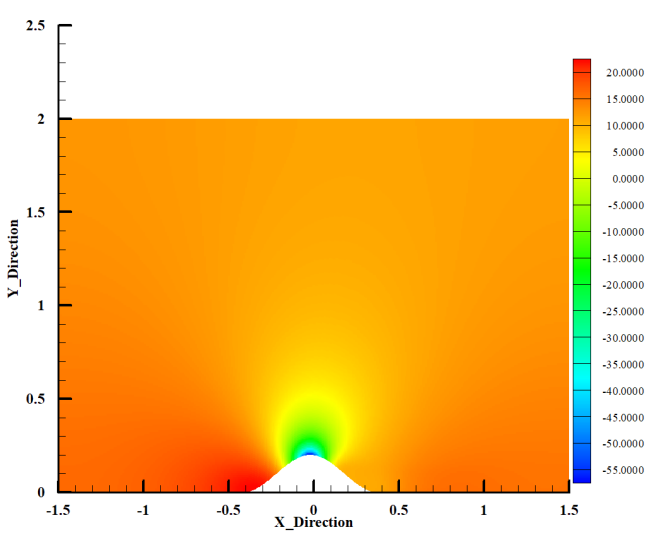


Fig. 9. Pressure contour

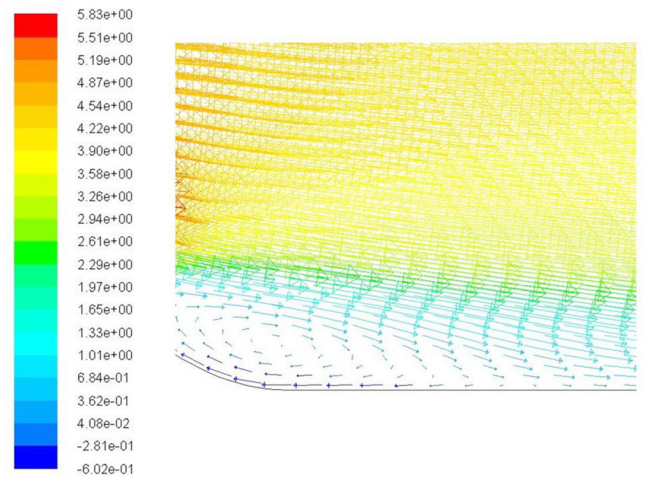


Fig. 11. Velocity vectors

The wind turbine performance installed in the mast point and in the point derived from the algorithm are compared. The wind turbine class is considered as IEC III Low Wind based on the wind condition in the studied region. Power estimation has been performed; Proven 15 kW, Rotor diameter 9 m, Rated power 15 kW, and Power regulation: Stall Control. According to the most recent table of American Wind Energy Association (AWEA), this region must be considered as a low capacity region. Wind power can be then calculated from Eq. (16).

$$P_r = \frac{1}{2} \times \rho \times A \times v^3 \times c_p \quad (16)$$

Where ρ , A , v and c_p refer to air density, swept area, free stream wind velocity and Betz limit respectively [32]. The calculated power output revealed to be 15 kW, therefore a 15 kW wind turbine with 9 meter rotor diameter was used to perform the comparison.

According to the above table power output at the point close to the top of the hill is almost nineteen times greater than the

Table 7. Comparison of output power of a 15 kW wind Turbine at two different location of a hill

At the leeside of the hill	$P_T=0.78$ kW
At the top of the hill	$P_T=14.99$ kW

one on the leeside of the hill, therefore installing the wind turbine in the leeside of the hill is absolutely inefficient. The effects of wind velocity on the turbine power output and electricity generated is clear according to the results of this paper.

5- Conclusion

In this study, the atmospheric boundary layer is numerically simulated using CFD coupled with inverse method in a mountainous terrain. The challenging issue was to determine the appropriate boundary conditions satisfying the atmospheric boundary layer. While in previous works, a uniform velocity profile was considered; herein a real velocity profile was employed based on the available meteorological

mast data. This novel approach leads to inverse solution. The optimization keeps correcting the velocity inlet profile until the velocity from the simulation is equal to the velocity recorded by the mast. It has been shown that coupling CFD simulation of atmosphere with inverse method provides more accurate results to determine velocity profile. The proposed method was implemented for 2-D geometry. Simulation results indicated that the optimum location to install a wind turbine is a point close to the summit and not the summit itself. Moreover, the appropriate wind turbine for this region has been selected.

Furthermore resultant pressure contours demonstrated that air flow pressure decreases over the hill and its minimum value is reported at the top of the hill, thus adverse pressure gradient happens in the back hill. It has been also proved that the inlet velocity converges to value of 3.16 m/s based on the optimization algorithm. It has also been shown that using a 15 kW wind turbine in the determined optimum point, results to nineteen times greater power output compared to the point of mast.

Nomenclature

Z_o	Effective surface roughness
g	standard gravity (m/s ²)
P	Power (Kw)
T	Time (s)
v	Velocity (m/s)
u	Velocity (m/s)
n	Power of Velocity changes with height
x	Length (m)
y	Height (m)
I	Identity matrix

Greek symbols

τ	Stress tensor
θ	optimization function Variable
φ	Vector of design variables
α_r	Change Step
μ	Dynamic viscosity (Pa s)
ρ	Density (kg/m ³)

Subscripts

ref	Reference point
inlet	Inlet
a	air
Mean	mean

References

[1] K. Kaygusuz, Wind energy: progress and potential, *Energy sources*, 26(2) (2004) 95-105.
 [2] M. Ritter, L. Deckert, Site assessment, turbine selection, and local feed-in tariffs through the wind energy index, *Applied Energy*, 185 (2017) 1087-1099.
 [3] P. Mittal, K. Mitra, Decomposition based multi-objective optimization to simultaneously determine the number

and the optimum locations of wind turbines in a wind farm, *IFAC-PapersOnLine*, 50(1) (2017) 159-164.

[4] T. Burton, N. Jenkins, D. Sharpe, E. Bossanyi, *Wind energy handbook*, John Wiley & Sons, 2011.
 [5] H. Cetinay, F.A. Kuipers, A.N. Guven, Optimal siting and sizing of wind farms, *Renewable Energy*, 101 (2017) 51-58.
 [6] S. Yan, S. Shi, X. Chen, X. Wang, L. Mao, X. Liu, Numerical simulations of flow interactions between steep hill terrain and large scale wind turbine, *Energy*, (2018).
 [7] C.J. Desmond, S.J. Watson, P.E. Hancock, Modelling the wind energy resource in complex terrain and atmospheres. Numerical simulation and wind tunnel investigation of non-neutral forest canopy flow, *Journal of Wind Engineering and Industrial Aerodynamics*, 166 (2017) 48-60.
 [8] A. Russell, *Computational fluid dynamics modeling of atmospheric flow applied to wind energy research*, (2009).
 [9] H. Ertürk, O.A. Ezekoye, J.R. Howell, Boundary condition design to heat a moving object at uniform transient temperature using inverse formulation, *Journal of manufacturing science and engineering*, 126(3) (2004) 619-626.
 [10] R. Mehdipour, A. Ashrafizadeh, K. Daun, C. Aghanajafi, Dynamic optimization of a radiation paint cure oven using the nominal cure point criterion, *Drying Technology*, 28(12) (2010) 1405-1415.
 [11] R. Mehdipour, C. Aghanajafi, A. Ashrafizadeh, Optimal design of radiation paint cure ovens using a novel objective function, *Pigment & Resin Technology*, 41(4) (2012) 240-250.
 [12] M.A. Mahmoud, A.E. Ben-Nakhi, Neural networks analysis of free laminar convection heat transfer in a partitioned enclosure, *Communications in Nonlinear Science and Numerical Simulation*, 12(7) (2007) 1265-1276.
 [13] H. Ertürk, O.A. Ezekoye, J.R. Howell, The Use of Inverse Formulation in Design and Control of Transient Radiant Systems, in: *Proceedings of International Heat Transfer Conference*, Grenoble, France, 2002.
 [14] F.H. França, O.A. Ezekoye, J.R. Howell, Inverse boundary design combining radiation and convection heat transfer, *Journal of heat transfer*, 123(5) (2001) 884-891.
 [15] J. Xiao, J. Li, Q. Xu, Y. Huang, H.H. Lou, ACS-based dynamic optimization for curing of polymeric coating, *AIChE journal*, 52(4) (2006) 1410-1422.
 [16] A. Ashrafizadeh, R. Mehdipour, C. Aghanajafi, A hybrid optimization algorithm for the thermal design of radiant paint cure ovens, *Applied Thermal Engineering*, 40 (2012) 56-63.
 [17] H.G. Kim, C.M. Lee, H.C. Lim, N.H. Kyong, An experimental and numerical study on the flow over two-dimensional hills, *Journal of Wind Engineering and Industrial Aerodynamics*, 66(1) (1997) 17-33.
 [18] H.G. Kim, V. Patel, C.M. Lee, Numerical simulation of

- wind flow over hilly terrain, *Journal of wind engineering and industrial aerodynamics*, 87(1) (2000) 45-60.
- [19] D. Fallo, *Wind energy resource evaluation in a site of central Italy by CFD simulations*, UNIVERSITÀ DEGLI STUDI DI CAGLIARI. Cagliari, Italia, (2007).
- [20] P. Fang, M. Gu, J. Tan, B. Zhao, D. Shao, *Modeling the neutral atmospheric boundary layer based on the standard $k-\epsilon$ turbulent model: modified wall function*, *Wind Engineering*, (2009).
- [21] S. Cao, T. Wang, Y. Ge, Y. Tamura, Numerical study on turbulent boundary layers over two-dimensional hills—effects of surface roughness and slope, *Journal of wind engineering and industrial aerodynamics*, 104 (2012) 342-349.
- [22] Z. Liu, T. Ishihara, T. Tanaka, X. He, LES study of turbulent flow fields over a smooth 3-D hill and a smooth 2-D ridge, *Journal of Wind Engineering and Industrial Aerodynamics*, 153 (2016) 1-12.
- [23] G. Mosetti, C. Poloni, B. Diviacco, Optimization of wind turbine positioning in large windfarms by means of a genetic algorithm, *Journal of Wind Engineering and Industrial Aerodynamics*, 51(1) (1994) 105-116.
- [24] S. Grady, M. Hussaini, M.M. Abdullah, Placement of wind turbines using genetic algorithms, *Renewable energy*, 30(2) (2005) 259-270.
- [25] A. Emami, P. Noghreh, New approach on optimization in placement of wind turbines within wind farm by genetic algorithms, *Renewable Energy*, 35(7) (2010) 1559-1564.
- [26] C. Wan, J. Wang, G. Yang, X. Li, X. Zhang, Optimal micro-siting of wind turbines by genetic algorithms based on improved wind and turbine models, in: *Decision and Control, 2009 held jointly with the 2009 28th Chinese Control Conference. CDC/CCC 2009. Proceedings of the 48th IEEE Conference on*, IEEE, 2009, pp. 5092-5096.
- [27] E. EU-FP, Wind loads on solar energy roofs, *Heron*, 52(3) (2007) 201.
- [28] Z. Baniamerian, R. Mehdipour, Studying Effects of Fence and Sheltering on the Aerodynamic Forces Experienced by Parabolic Trough Solar Collectors, *Journal of Fluids Engineering*, 139(3) (2017) 031103.
- [29] J.A. Peterka, Z. Tan, B. Bienkiewicz, J. Cermak, Wind loads on heliostats and parabolic dish collectors: Final subcontractor report, *Solar Energy Research Inst.*, Golden, CO (USA), 1988.
- [30] A. Ashrafizadeh, G.D. Raithby, G. Stubbley, Direct design of shape, *Numerical Heat Transfer: Part B: Fundamentals*, 41(6) (2002) 501-520.
- [31] K. Daun, H. Erturk, J.R. Howell, Inverse design methods for high-temperature systems, *Arabian Journal for Science and Engineering*, 27(2) (2002) 3-48.
- [32] M. Zanganeh, V. Khalajzadeh, Validation of the WAsP model for a terrain surrounded by mountainous region, in: *Proceedings of World Academy of Science, Engineering and Technology*, 2011, pp. 379-383.

Please cite this article using:

A. H. Zare, R. Mehdipour, E. Mohammadi, Determining a Suitable Location for Wind Turbines Using Inverse Solution and Mast Data in a Mountainous Terrain, *AUT J. Mech. Eng.*, 2(2) (2018) 243-252.

DOI: 10.22060/ajme.2018.13813.5319

